



The formulation of metakaolin-based aluminosilicate geopolymer for spray coating

Pattarasuda Viensiri, Suthee Wattanasiriwech, Anucha Wannagon, and Darunee Wattanasiriwech*

Department of Materials innovation, School of Science, Mae Fah Luang University,
Chiang Rai, Thailand

*Corresponding author, E-mail: darunee@mfu.ac.th

Abstract

Geopolymer coating was prepared from metakaolin-based aluminosilicate for the formulation of spray. The effects of Si/Al ratios on the properties of the slurry were investigated using X-ray diffraction measurements (XRD), Fourier-transform infrared spectroscopy (FTIR), viscometry, and scanning electron microscopes (SEM). The results showed the geopolymer slurry with Si/Al molar ratios of 1:5, 1:6, and 1:7 had viscosity appropriate for spraying. All the geopolymer specimens were amorphous phase. The FTIR pattern showed the Si-O-Si bonds from geopolymerization in all geopolymer specimens. The spray slurry with a Si/Al molar ratio of 1:7 was found to be suitable for coating. The thickness of the coating layer (3-4 layers) was around 60-80 micrometers.

Keywords: *Geopolymer, Metakaolin, Spray coating*

1. Introduction

Geopolymer coating, a class of new inorganic coatings, has been investigated and applied to the surface protection of concrete, steel, and wood structural elements (Jiang et al., 2020). Geopolymer is a crosslink aluminosilicate structure synthesized by the chemical reaction (geopolymerization) of an aluminosilicate powder with an alkaline solution. The geopolymer has the potential for protective coatings for different surfaces including metal and concrete due to their superior mechanical, long-term performance, and fire resistance properties (Wang et al., 2019).

One of the primary mechanisms of deterioration of reinforced concrete exposed to environments containing primarily chloride ions and or carbon dioxide is corrosion of reinforcing steel (Aguirre-Guerrero et al., 2017). Carbon dioxide in the air forms an acid solution in moist environments, which can react with the hydrated cement paste and tends to neutralize the alkalinity of concrete (This is referred to as the carbonation process) (Bertolini et al., 2013). Carbonation has a significant impact on the corrosion of embedded steel. The first effect is that the pH of the pore solution decreases from its normal range of pH 13 to 14 to values close to neutral (Bertolini et al., 2013). Currently, coating materials could be divided into two types; inorganic and organic treatments (Pan et al., 2017). Coating materials could be divided into two types; inorganic and organic (Pan et al., 2017). An organic coating is most commonly used due to its good protective performance. However, there are concerns about limited-service life and instability under UV radiation. The most common inorganic surface treatment is sodium silicate solution, also known as a water glass (Pan et al., 2017). To a much smaller extent, potassium silicates, lithium silicates, and fluosilicates have also been reported to be used as inorganic surface treatments (Pan et al., 2017).

Several coating methods can be used, such as dipping (Temuujin et al., 2010), spraying (Temuujin et al., 2012), and also painting (Deshmukh et al., 2017). However, by spraying, a strong uniform thickness of the coating can be controlled and applied to a substrate that is complicated shape. The ease with which geopolymer can be applied onto substrate surfaces depends on the water content formulation (Sufian et al., 2018). The rheology and viscosity of slurry that is appropriate for coating are important parameters. The aim of this research focuses on studying geopolymer coating-based metakaolin by spray technique to develop the suitable geopolymer formulations for coating on concrete substrates with testing properties of geopolymer slurry, including viscosity, setting time, and the thickness of the microstructure of the slurry was investigated.

[475]



2. Objectives

1. To study metakaolin-based geopolymer coating by varying the molar ratio of Si/Al from 1.0-2.0 and Na/Al = 1, then selection of slurry conditions as appropriate for spray coating.
2. To study the appropriate thickness of geopolymer slurry for spray coating on concrete.

3. Materials and Methods

3.1 Materials

The aluminosilicate source used was metakaolin (Chemius Korea, Korea), calcined at 1000°C for 1h. The analysis of the chemical compositions using an X-ray fluorescence (XRF) technique is presented in Table 1. Alkali activator is a combination of sodium hydroxide (NaOH) and sodium silicate (Na₂SiO₃). NaOH pellets using AR grade which was supplied by QReC, New Zealand (99% purity) while Na₂SiO₃ is available commercially in solution form with the chemical composition of Na₂O is 16.50%, SiO₂ is 35.25% and H₂O is 48.25% were acquired from C. THAI CHEMICALS CO., LTD. Concrete substrate was cement mortar for slurry coating, cement mortar used consists of 1 part cement and 2.75 parts of sand proportioned by mass according to ASTM C109 (ASTM C109/C109M-02, 2020).

Table 1 Chemical composition of the metakaolin and sodium silicate.

Materials	SiO ₂	Al ₂ O ₃	Fe ₂ O ₃	TiO ₂	CaO	Na ₂ O	K ₂ O	H ₂ O
Metakaolin	52.1	45.3	0.60	1.64	0.05	0.21	0.16	-
Sodium silicate	35.25	-	-	-	-	16.50	-	48.25

3.2 Geopolymer spray preparation

The geopolymer spray was mainly prepared from metakaolin and alkali activator (sodium hydroxide (4 Molar) and sodium silicate). The Na/Al was fixed at 1 and Si/Al molar ratios were given in Table 2. Prior to use, the alkali activators, Na₂SiO₃ and NaOH, were mixed. The mixed activator was poured into a beaker containing metakaolin, and the mixture was mixed for 2 minutes with a mixer to ensure that the slurry was well mixed. The slurry was sprayed on a concrete substrate with a dimension of 15×15 cm used by a spray gun. The coating interval between each layer was 3 minutes and the coating was 5 layers.

Table 2 Geopolymer slurry coating composition.

Codes	M1:0	M1:1	M1:2	M1:3	M1:4	M1:5	M1:6	M1:7	M1:8	M1:9	M2:0
Si/Al	1	1.1	1.2	1.3	1.4	1.5	1.6	1.7	1.8	1.9	2.0
Na/Al	1	1	1	1	1	1	1	1	1	1	1

3.3 Characterization

Phase compositions of the metakaolin and geopolymer slurry were investigated using X-ray diffraction (XRD, PANalytical, X'pertPro). Fourier Transform Infrared (FTIR, Thermo scientific/Nicolet is50) with a scanning range from 400 to 4000 cm⁻¹ by geopolymer slurry was performed into powder and then mixed with potassium bromide (KBr). The thickness of the coating was determined using an optical microscope. The morphology of metakaolin particles in Figure 1. and geopolymer slurry was observed using a Scanning Electron Microscope (SEM, Tescan MIRA4). Before being characterized with the SEM method, the geopolymer coating specimens were molded with epoxy resin.

The setting time of geopolymer was measured following ASTM C191 (ASTM C191, 2008) using the Vicat needle. The geopolymer was poured into a PVC cylindrical mold, and then the initial and final setting times were determined. The viscosity of the slurry was measured following ASTM D2487 (ASTM D 4287-00, 2019) using a viscosity meter.

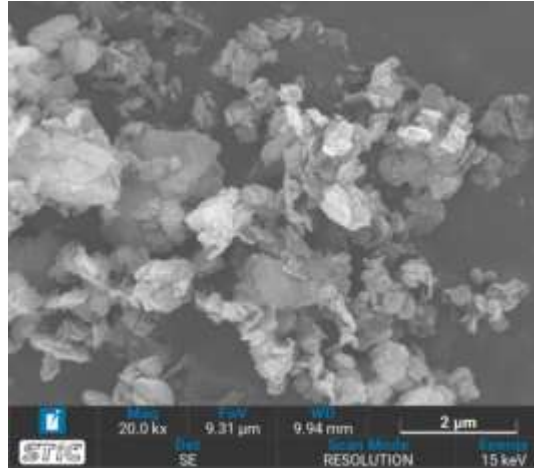


Figure 1 SEM showed morphology of metakaolin particles.

4. Results and Discussion

4.1 Viscosity and setting time

The result of the setting time of the geopolymer coating is shown in Figure 2.

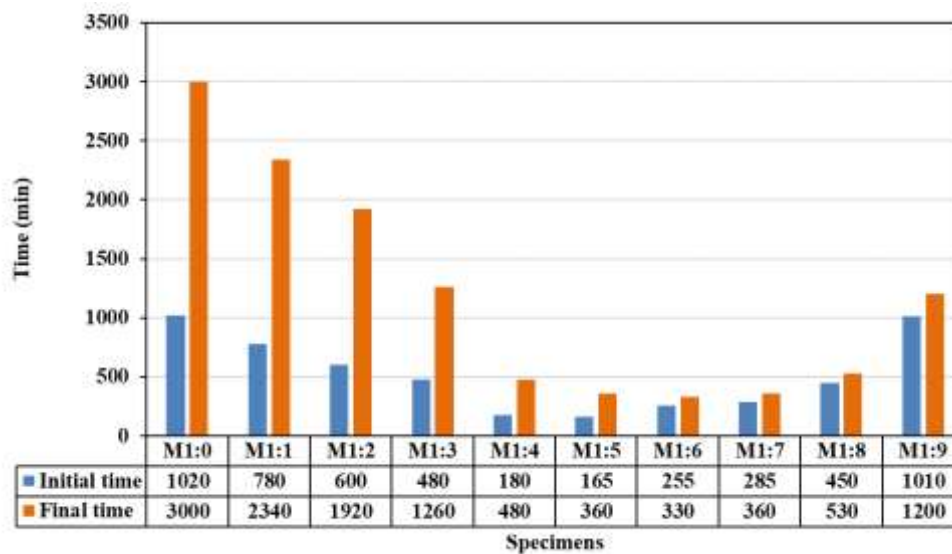


Figure 2 The setting time of geopolymer slurry.

It shows the decreasing trend of each specimen as the Si/Al ratio was increased from M1:0, M1:1, M1:2, M1:3, M1:4, M1:5, and M1:6. Further increased Si/Al ratio in M1:7, M1:8, and M1:9, viscosity was increased again. However, with the specimen with the Si/Al = 2 (M2:0), the mixing was unsuccessful because the Na^+ ion from sodium hydroxide was insufficient to dissolve metakaolin.

The viscosity testing was recorded at 5 min after mixing the raw materials for 2 min. The result is shown in Figure 3. It had the same trend as setting time (final setting time). The viscosity of the slurry had sharply as the Si/Al ratio was increased in the period from M1:5 - M1:7 because in this region the geopolymerization and setting occur quickly. The viscosity of the slurry for spray coating should not exceed

[477]



1 Pa.s according to the standard of ASTM D4287. Our M1:5, M1:6, and M1:7 recipes thus passed this standard. After M1:8 and M1:9, there was increased viscosity due to an increase in the Si/Al molar ratio. Because the increase in sodium silicate caused increased viscosity and sodium hydroxide decreased, it was insufficient to dissolve metakaolin.

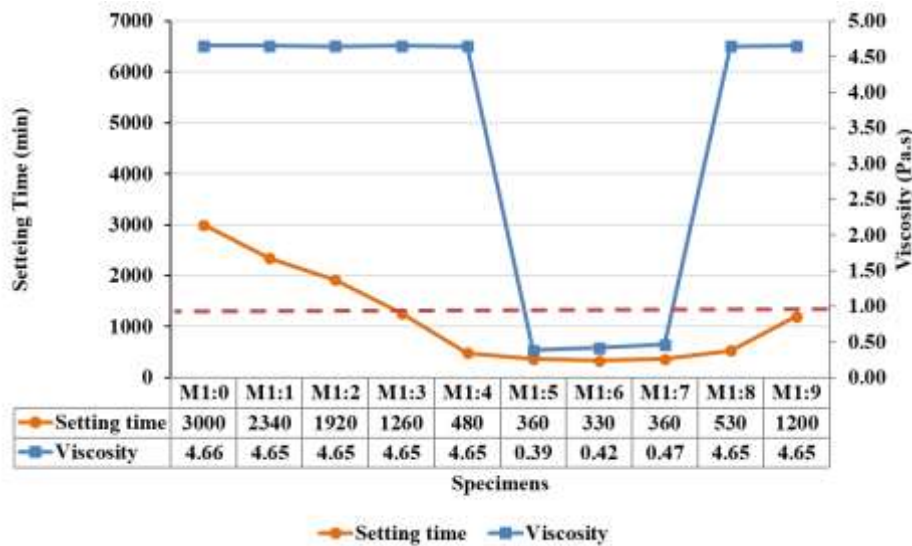


Figure 3 The viscosity and setting time of geopolymer coating.

4.2 XRD result

Phase identification of metakaolin (MK) and geopolymers spray slurry with Si/Al ratios of 1.5 (M1:5), 1.6 (M1:6), and 1.7 (M1:7) is shown in Figure 4.

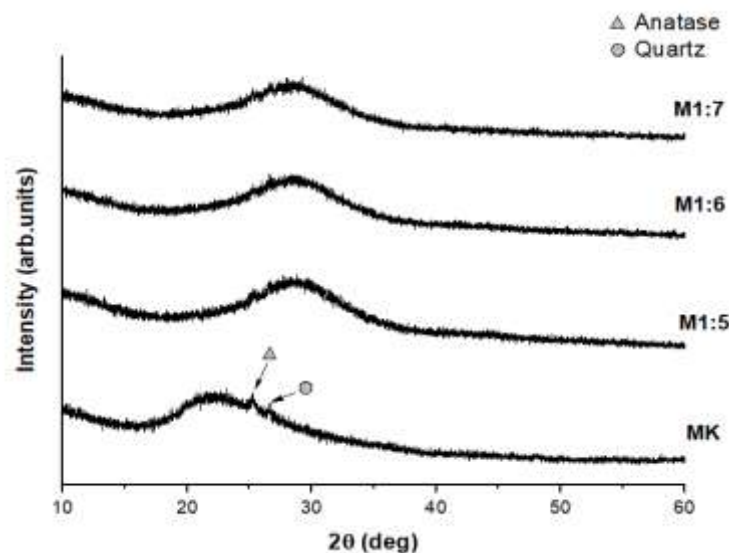


Figure 4 XRD patterns for each condition of geopolymer coating



It was noted that MK showed a typical amorphous phase with the existence of anatase at 25.3° and quartz at 26.6° . When the Si/Al ratio had increased, the amorphous phase observed in M 1:5, M 1:6, and M 1:7 was exposed clearly. It shows that when the Si/Al ratio increased, geopolymers displayed varying degrees of geopolymerization, which would be discussed using FTIR analysis.

4.3 FTIR analysis

The FTIR results of specimens are shown in Figure 5.

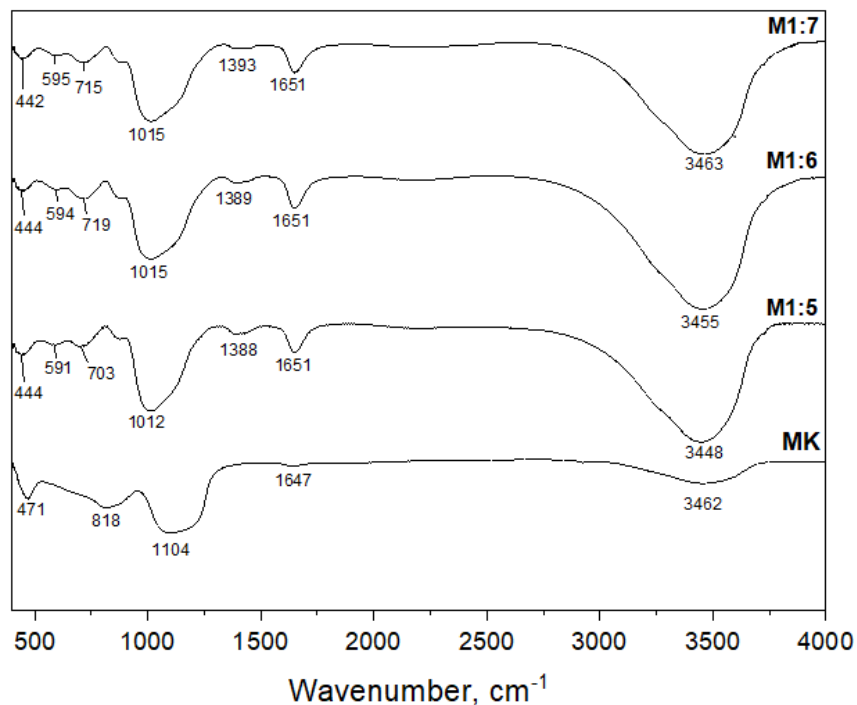


Figure 5 FTIR spectra of geopolimer coating of each condition.

The metakaolin (MK) showed several peaks centered at $3,462$, $1,647$, $1,104$, 818 , and 471 cm^{-1} . The broad peak at $3,462$ cm^{-1} and a weak peak at $1,647$ cm^{-1} are due to the stretching vibrations of O-H bonds and H-O-H bending vibrations of interlayer adsorbed H_2O molecule, respectively (Kumar et al., 2015). The main peaks of metakaolin are at $1,104$, 818 , and 471 cm^{-1} , corresponding to the asymmetrical stretching vibration of Si-O-Si bonds, stretching vibrations of the Si-O-Al, and bending vibration of Si-O, respectively (Gao et al., 2020). After geopolymerization, the typical peak related to the asymmetrical stretching vibration of Si-O-T (T was Si or Al) bonds at $1,388$ - $1,393$ cm^{-1} (Irfan Khan et al., 2014) and $1,012$ - $1,015$ cm^{-1} in metakaolin shifted to lower frequencies (M1:5, M1:6, and M1:7 specimens) (He et al., 2016); (Mao et al., 2020). During the geopolymerization reaction, there was a noticeable change in the functional groups of both Al and Si, resulting in the production of new products with a different chemical environment than metakaolin (He et al., 2016). Therefore, the peaks at 703 - 719 cm^{-1} are symmetrical stretching vibration of Si-O bonds, the peaks at 591 - 595 cm^{-1} are bending vibration of Si-O-Al and the peaks at 442 - 444 cm^{-1} are bending vibration of Si-O (He et al., 2016).



4.4 The coating

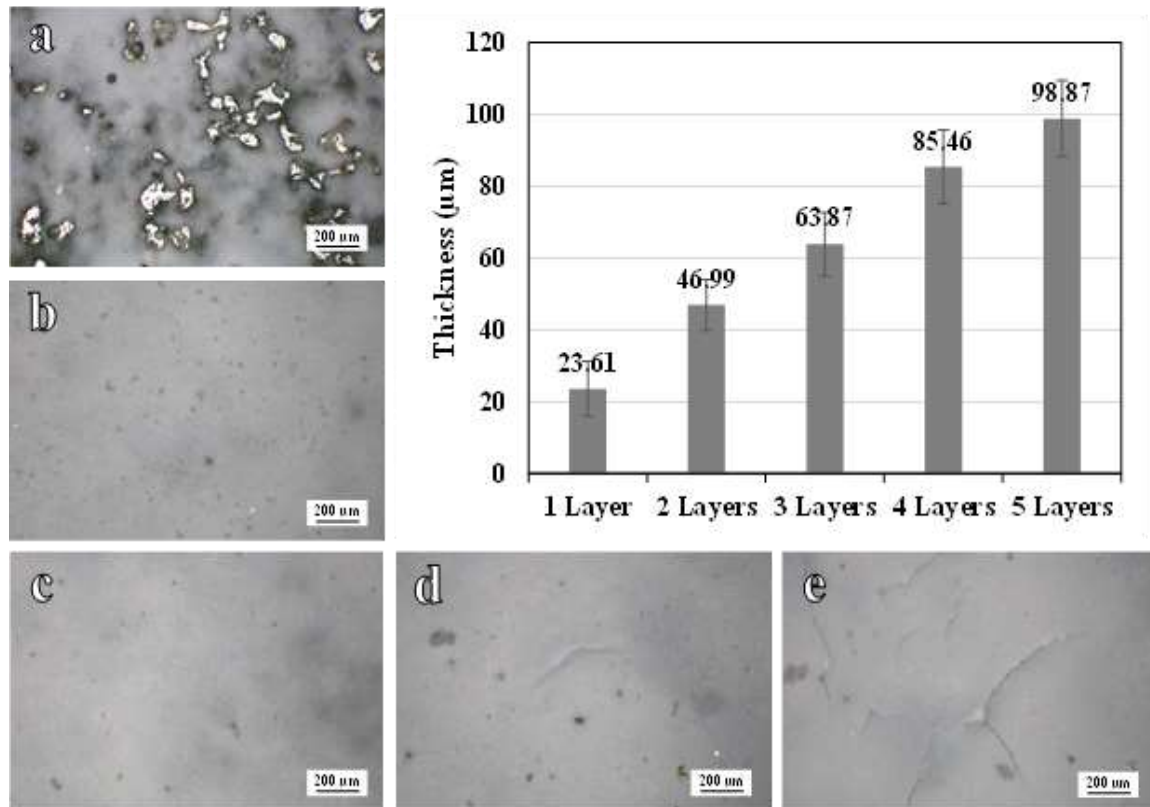


Figure 6 The surface after each coating layer using M1:7 spray slurry; a) 1 layer, b) 2 layers, c) 3 layers, d) 4 layers and e) 5 layers; the graph shows the thickness of coating at various layers

From the experiment, the slurry of M1:5, M1:6, and M1:7 was spray coated on the concrete substrate. Coatings with M1:5 and M1:6 had cracking across the coating surface after drying. Due to drying shrinkage as the slurries had higher water contents. The M1:7 specimen had some cracks around the edges. This had the least cracks due to the lower drying shrinkage. In M1:5 and M1:6, there was more sodium hydroxide in the slurry than in the M1:7 specimen. The M1:7 formulation was then selected for further investigation of the thickness of coating layers. The surface of each layer is shown in Figure 6. After the first coating, there were areas of non-uniform thickness due to insufficient coating Figure 6 (a). After the second and third coatings, the surface becomes smoother with a coating thickness of around 58.43 and 63.51 μm , respectively. No visible crack on the surface due to sufficient to coating Figure 6 (b and c). After the fourth coating, a few wrinkles were observed with a thickness of around 82.88 μm , the layer had no cracks on the surface Figure 6 (d). After the fifth coating, obvious cracks were observed with a thickness of around 98.82 μm Figure 6 (e). The morphology of the geopolymer coating layer is shown cross-section in Figure 7. The bonding interface between the geopolymer slurry and the concrete substrate was complex and tightly bound.

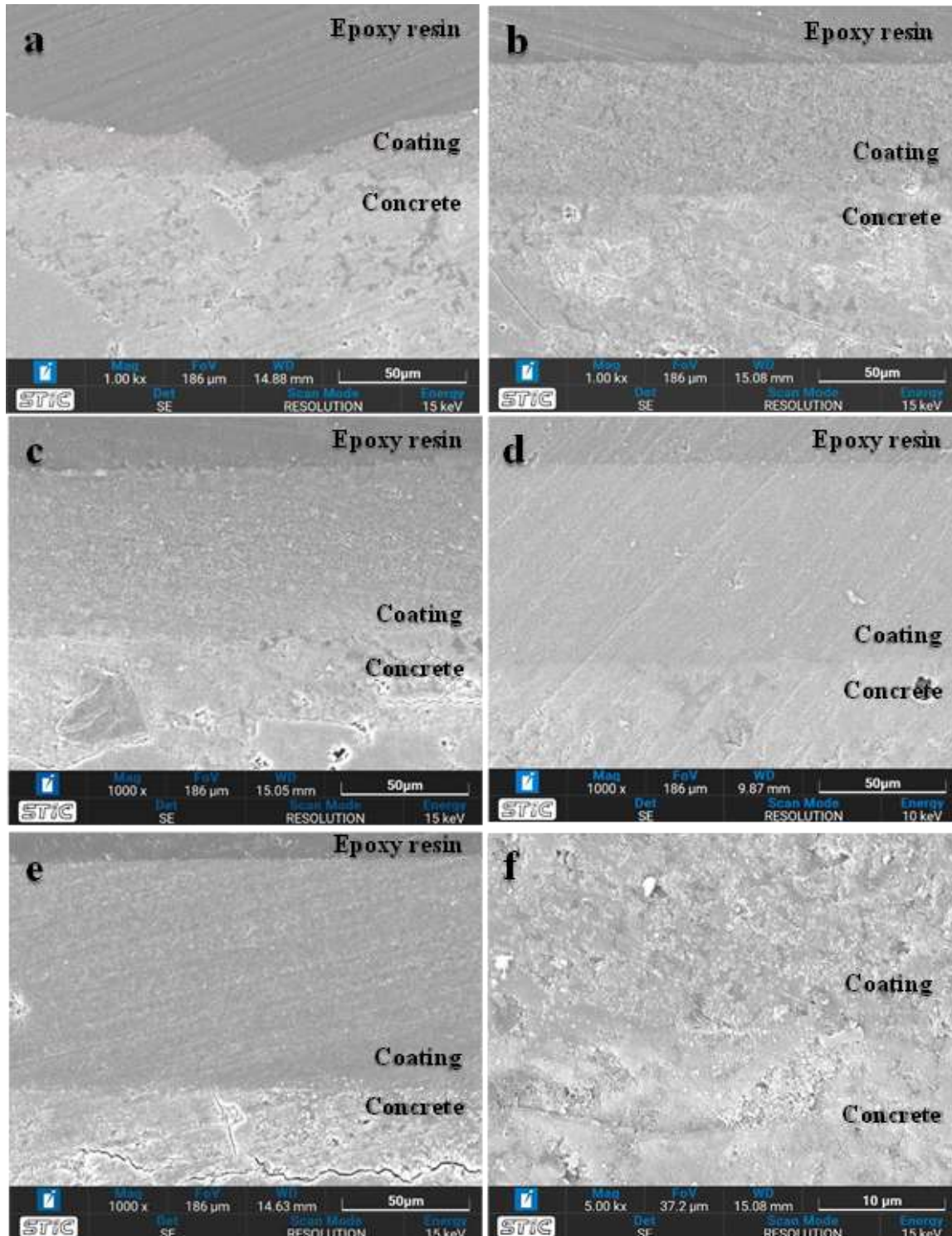


Figure 7 SEM morphology of cross-section of geopolymer slurry; a) 1 layer, b) 2 layers, c) 3 layers, d) 4 layers and e) 5 layers and f) the interface between the geopolymer slurry and the concrete substrate.



5. Conclusion

The formulation of geopolymer for spray coating with different Si/Al ratios was prepared by mixing alkaline silicate solution and metakaolin. Effects of Si/Al ratio on the viscosity, structure, and mechanical properties. The main conclusions could be drawn as below:

1. The appropriate viscosity of the slurry for spray coating according to ASTM following was at Si/Al of 1:5, 1:6, and 1:7.
2. All the geopolymers coating showed an amorphous phase with the functional group of asymmetrical stretching vibration of Si–O–T bonds.
3. The thickness of the coating layer is appropriate around 3-4 layers with a thickness of around 60-80 μm .

6. Acknowledgements

The authors are grateful for the financial support from the Thailand Graduate Institute of Science and Technology (TGIST) scholarship, the National Science and Technology Development Agency (NSTDA), Thailand. Furthermore, research funding provided by Mae Fah Luang University is highly appreciated.

7. References

- Aguirre-Guerrero, A. M., Robayo-Salazar, R. A., & de Gutiérrez, R. M. (2017). A novel geopolymer application: Coatings to protect reinforced concrete against corrosion. *Applied Clay Science*, *135*, 437–446. <https://doi.org/10.1016/j.clay.2016.10.029>
- ASTM C109/C109M-02. (2020). Standard Test Method for Compressive Strength of Hydraulic Cement Mortars. *Annual Book of ASTM Standards*, *04*, 9.
- ASTM C191. (2008). Time of Setting of Hydraulic Cement by Vicat Needle ASTM C-191. *Annual Book of ASTM Standards*, *191-04*, 1–10.
- ASTM D 4287-00. (2019). *Standard Test Method for High-Shear Viscosity Using a Cone/Plate Viscometer*. *06.01*, 4. <https://doi.org/10.1520/mnl10913m>
- Bertolini, L., Elsener, B., Pedferri, P., Redaelli, E., & Polder, R. B. (2013). Chapter 5: Carbonation induced corrosion. In *Corrosion of Steel in Concrete: Prevention, Diagnosis, Repair, 2nd edition*. (pp. 79–92). Wiley-VCH Verlag GmbH & Co, Weinheim. <https://doi.org/10.1002/9783527651696.ch5>
- Deshmukh, K., Parsai, R., Anshul, A., Singh, A., Bharadwaj, P., Gupta, R., Mishra, D., & Sitaram Amritphale, S. (2017). Studies on fly ash based geopolymeric material for coating on mild steel by paint brush technique. *International Journal of Adhesion and Adhesives*, *75*, 139–144. <https://doi.org/10.1016/j.ijadhadh.2017.03.002>
- Gao, L., Zheng, Y., Tang, Y., Yu, J., Yu, X., & Liu, B. (2020). Effect of phosphoric acid content on the microstructure and compressive strength of phosphoric acid-based metakaolin geopolymers. *Heliyon*, *6*(4), e03853. <https://doi.org/10.1016/j.heliyon.2020.e03853>
- He, P., Wang, M., Fu, S., Jia, D., Yan, S., Yuan, J., Xu, J., Wang, P., & Zhou, Y. (2016). Effects of Si/Al ratio on the structure and properties of metakaolin based geopolymer. *Ceramics International*, *42*(13), 14416–14422. <https://doi.org/10.1016/j.ceramint.2016.06.033>
- Irfan Khan, M., Azizli, K., Sufian, S., & Man, Z. (2014). Effect of Na/Al and Si/Al ratios on adhesion strength of geopolymers as coating material. *Applied Mechanics and Materials*, *625*, 85–89. <https://doi.org/10.4028/www.scientific.net/AMM.625.85>
- Jiang, C., Wang, A., Bao, X., Ni, T., & Ling, J. (2020). A review on geopolymer in potential coating application: Materials, preparation and basic properties. *Journal of Building Engineering*, *32*(September), 101734. <https://doi.org/10.1016/j.jobbe.2020.101734>
- Kumar, S., Kristály, F., & Mucsi, G. (2015). Geopolymerisation behaviour of size fractioned fly ash. *Advanced Powder Technology*, *26*(1), 24–30. <https://doi.org/10.1016/j.appt.2014.09.001>



- Mao, Y., Biasetto, L., & Colombo, P. (2020). Metakaolin-based geopolymer coatings on metals by airbrush spray deposition. *Journal of Coatings Technology and Research*, 17(4), 991–1002.
<https://doi.org/10.1007/s11998-019-00310-6>
- Pan, X., Shi, Z., Shi, C., Ling, T. C., & Li, N. (2017). A review on concrete surface treatment Part I: Types and mechanisms. *Construction and Building Materials*, 132, 578–590.
<https://doi.org/10.1016/j.conbuildmat.2016.12.025>
- Sufian, S., Mat Yakob, S., Rabat, N. E., & Md Zin, R. (2018). Review on Geopolymer As a New Green Coating Material. *Journal of Industrial Technology*, 26(1), 59–73.
<https://doi.org/10.21908/jit.2018.2>
- Temuujin, J., Minjigmaa, A., Rickard, W., Lee, M., Williams, I., & van Riessen, A. (2010). Fly ash based geopolymer thin coatings on metal substrates and its thermal evaluation. *Journal of Hazardous Materials*, 180(1–3), 748–752. <https://doi.org/10.1016/j.jhazmat.2010.04.121>
- Temuujin, J., Minjigmaa, A., Rickard, W., & Van Riessen, A. (2012). Thermal properties of spray-coated geopolymer-type compositions. *Journal of Thermal Analysis and Calorimetry*, 107(1), 287–292.
<https://doi.org/10.1007/s10973-011-1766-4>
- Wang, Y. S., Alrefaei, Y., & Dai, J. G. (2019). Silico-aluminophosphate and alkali-aluminosilicate geopolymers: A comparative review. *Frontiers in Materials*, 6(May), 1–17.
<https://doi.org/10.3389/fmats.2019.00106>